



**HAL**  
open science

## Mechanical and physical properties of flexible polyurethane foam filled with waste tire material recycles

Y Nezili, I El Aboudi, D He, A Mdarhri, C Brosseau, M Zaghrioui, T Chartier, A Ghorbal, R Ben Arfi, J Bai

### ► To cite this version:

Y Nezili, I El Aboudi, D He, A Mdarhri, C Brosseau, et al.. Mechanical and physical properties of flexible polyurethane foam filled with waste tire material recycles. *Journal of Applied Polymer Science*, 2024, 10.1002/app.56282 . hal-04730899

**HAL Id: hal-04730899**

**<https://hal.univ-brest.fr/hal-04730899v1>**

Submitted on 10 Oct 2024


**HAL** is a multi-disciplinary open access archive for the deposit and dissemination of scientific research documents, whether they are published or not. The documents may come from teaching and research institutions in France or abroad, or from public or private research centers.

L'archive ouverte pluridisciplinaire **HAL**, est destinée au dépôt et à la diffusion de documents scientifiques de niveau recherche, publiés ou non, émanant des établissements d'enseignement et de recherche français ou étrangers, des laboratoires publics ou privés.



Distributed under a Creative Commons Attribution - NonCommercial 4.0 International License

# Mechanical and physical properties of flexible polyurethane foam filled with waste tire material recycles

Y. Nezili<sup>1</sup> | I. El Aboudi<sup>1</sup> | D. He<sup>2</sup> | A. Mdarhri<sup>1</sup> | C. Brosseau<sup>3</sup>  |  
M. Zaghrioui<sup>4</sup> | T. Chartier<sup>4</sup> | A. Ghorbal<sup>5</sup> | R. Ben Arfi<sup>5</sup> | J. Bai<sup>2</sup>

<sup>1</sup>Laboratoire de Recherche en Développement Durable & Santé-FSTG, A. El Khattabi, Univ. Cadi Ayyad, Marrakech, Morocco

<sup>2</sup>LMPS-Laboratoire de Mécanique Paris-Saclay, Univ. Paris-Saclay, Centrale-Supélec, ENS Paris-Saclay, CNRS, Gif-sur-Yvette, France

<sup>3</sup>Lab-STICC, Univ. Brest, CNRS, Brest, France

<sup>4</sup>Laboratoire GREMAN, Univ. de Tours, Blois, France

<sup>5</sup>Research Unit Advanced Materials, Applied Mechanics, Innovative Processes, and Environment, UR22ES04, Higher Institute of Applied Sciences and Technology of Gabes, University of Gabes, Tunisia

## Correspondence

C. Brosseau, Lab-STICC, Univ. Brest, CNRS, CS 93837, 6 Avenue Le Gorgeu, 29238, Brest, Cedex 3, France.  
Email: [brosseau@univ-brest.fr](mailto:brosseau@univ-brest.fr)

## Funding information

Ministère de l'Enseignement Supérieur, de la Coopération Scientifique et de l'Innovation, Grant/Award Number: AUF 2021 N° DRM-6871; Agence Universitaire Francophone

## Abstract

In this work we use ground tire rubber (GTR) powder obtained by grinding worn tire treads as reinforcer agent in flexible polyurethane (PU). Characterization of the microstructure of the as-received powder is achieved using a series of standard techniques including scanning electron microscopy (SEM), granulometry-laser, Fourier transform infrared spectroscopy (FTIR), and x-ray diffraction (XRD). To have complementary physical information the composition and thermal characteristics of the GTR powder, thermogravimetry analysis (TGA) is also performed. The set of these preliminary characterizations shows that the GTR powder particles can be used as reinforcing fillers. For the purpose of good compatibility with the PU matrix, the GTR powder is subjected to chemical treatments for reducing the impurities on the powder particles and to create functional groups at their surface. Subsequently, a series of GTR/PU composite samples are prepared with different weight fractions of GTR using free rising foam method. The GTR/PU composites are then characterized to assess the effect of the GTR content and their chemically pre-treatment on thermal stability, compression mechanical behavior as well as sound attenuation properties. Collectively, these results indicate a significant improvement of both thermal and mechanical properties of the GTR/PU composites compared to the pristine PU matrix. Furthermore, it is also emphasized that the sound absorption response shows a significant shift of the maximum of the absorption coefficient toward lower frequencies resulting from simultaneous increase in air-flow resistivity and tortuosity which can have great potential application in the field of underwater acoustics. The effects of chemical treatments and GTR amount are also discussed. It is also shown that the results show improvement when H<sub>2</sub>O<sub>2</sub> solvent is used in comparison with NaOH, and the optimal properties are reached for PU samples containing 20 wt% of GTR whatever the pre-treatment is.

## KEYWORDS

composites, mechanical properties, structure-property relationships, thermal properties

This is an open access article under the terms of the [Creative Commons Attribution](https://creativecommons.org/licenses/by/4.0/) License, which permits use, distribution and reproduction in any medium, provided the original work is properly cited.

© 2024 The Author(s). *Journal of Applied Polymer Science* published by Wiley Periodicals LLC.

## 1 | INTRODUCTION AND BACKGROUND

Since engineering materials usually operate under either static or cyclic mechanical loads at specific environmental conditions, their performances evolve with time and several detrimental effects (e.g. cracks, cavities, agglomerates, voids) lead to damage accumulation, time and/or thermal aging, and premature fatigue resulting eventually to their failure.<sup>1</sup> When these engineering materials reach their end life, the management and disposal of the resulting waste becomes a top priority dictated by environmental sustainability, economic as well as social issues.<sup>2</sup> In,<sup>3</sup> Yang and coworkers highlighted the roles of identification and classification of recyclable waste as the premise for its reuse and energy consumption. Currently, recycling of waste rubber from tires is of utmost importance. In 2019, the end-of-life tires (ELTs) waste is estimated as 31 million tons worldwide and the actual trend predicts that it will increase by 20% in 2030.<sup>4,5</sup> In addition, the complex structure (tread depth, sidewall, belts, bead, inner liner, carcass) and composition (rubber, curing system, reinforcing fillers, textile fibers, steel oil, beads, antioxidants/ozonates) makes tires non-biodegradable materials. ELTs data reported by WBCSD-Global ELT Management show only 59% of end-of-life tires are correctly disposed while 41% are landfilled, stockpiled, or even lost.<sup>5</sup> The land disposal of plastic wastes is one of the main sources of debris/microplastics which are considered as major pollutants due to their significant impact in natural ecosystems.<sup>6</sup> It should, perhaps, be emphasized in this context that the accumulation of used tires in landfills poses a real environmental risk, such as exposure to sudden fires which release toxic gases into the atmosphere, as well as fluids from combustion. These fluids explicitly affect both fauna and flora. Some work has been done on addressing these concerns and various ways of recycling used tires including mechanical recycling, devulcanization, incineration, pyrolysis and retreading have been suggested.<sup>7</sup> Recycling of waste rubber from tires involves reduction of tire rubber into smaller particle size referred to as crumb rubber which can be used in several applications.<sup>4,8–10</sup>

In this study, waste tire material recycles are processed by using mechanical grinding operating at ambient temperature. Basically, it consists on a mechanical decomposition transforming the used tire into a powder to form ground tire rubber (GTR) available according to particle size: chips (10–50 mm), granules (1–10 mm), and powders (1 mm).<sup>11,12</sup> The mechanical decomposition is then followed by purification and elimination of both steel and textile lightweight fibrils components by a combination of shaking screens and wind sifters.<sup>13</sup> Due to

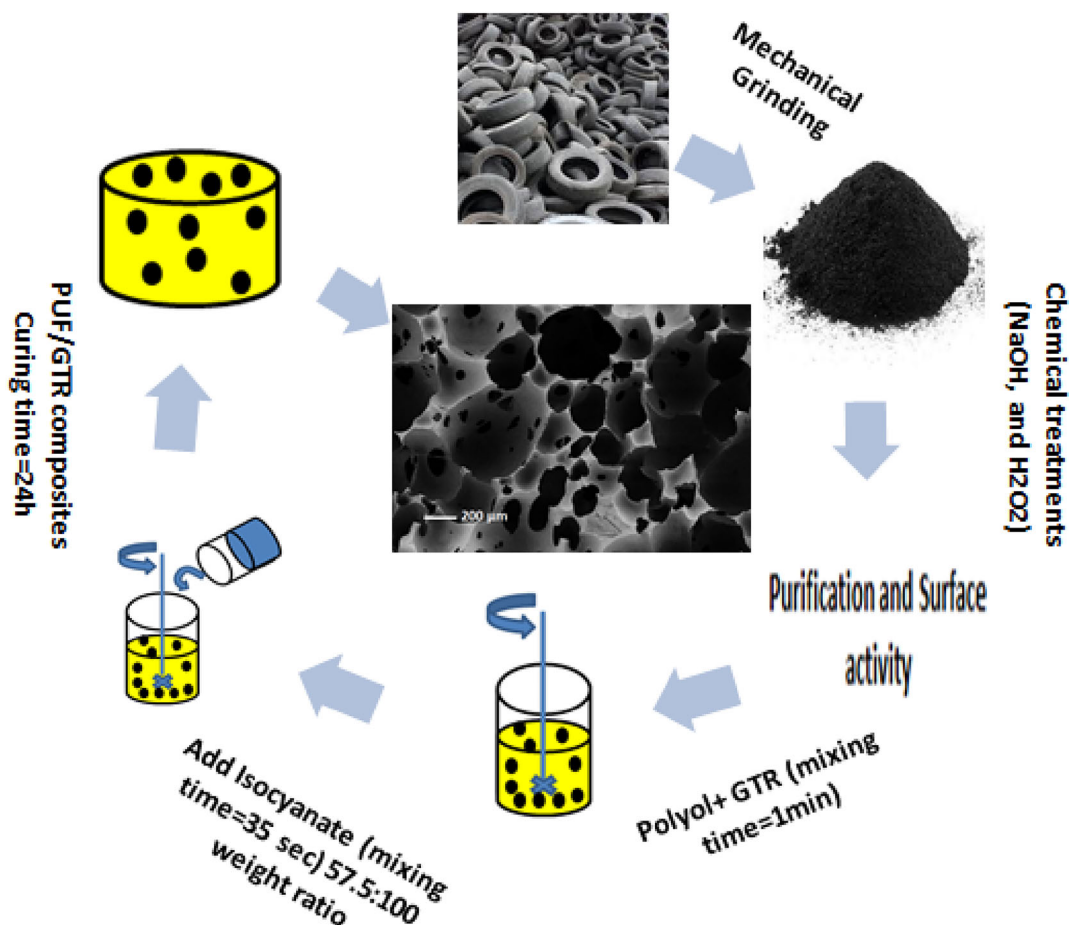
friction created by the force applied by knives used in grinding technology, heat is generated affecting thus the physical properties of recuperated rubber, for example increase in the degree of oxidation.<sup>12,14</sup> The residue extracted by grinded waste tires can be used as second material raw or as a reinforcement agent in pristine polymers to enhance their physical and/or mechanical properties.<sup>15–17</sup> For example, Ubaidillah and coworkers<sup>18</sup> studied how the mixing of GTR with variable content of magnetite can lead to a new class of high damping magneto-rheological elastomer which can be used as seismic shock absorbers or in the automotive industry.

Thanks to its excellent properties (hardness, strength, and modulus) and low production cost, PU foam is one of the most versatile materials due to the numerous applications in many industrial branches, for example in biomedical, building, and construction, textile.<sup>19</sup> Depending on its cellular structure, two kinds of PU foam can be distinguished: rigid and flexible foams. Incorporating the GTR into flexible polyurethane (PU) foams leads to an enhancement of its physical and in particular mechanical properties.<sup>10,20</sup> For example, Cerny and Jancar<sup>21</sup> investigated composite materials consisting of blending crumb rubber, with particle size ranging from 0.8 to 3 mm, in a polyurethane-urea (PUU) matrix. These authors found that the mechanical characteristics of the composite material are maximum when the filler content is between 50% and 65% by volume. They also concluded that the difference in adhesion between the matrix and the filler particles can motivate their use for in pavement maintenance and road repairs. In a different context,<sup>22</sup> it was suggested that the adding artichoke stem waste fibers in PU foam can lead to good mechanical and thermal/sound insulation performances, especially for low frequency sound absorption. In another study, Kosmela and coworkers<sup>23</sup> employed thermo-mechanical treatment of GTR involving fresh or waste rapeseed oils and reactive extrusion to produce flexible foamed PU composites. Both types of oil enhance the thermal stability of PU/GTR composites. Oil-induced GTR particle swelling increases the surface tension resulting in reduced cell size and increased closed cell content in the PU composites. Additionally, waste oil increases both compressive and tensile strengths by enhancing the interfacial adhesion between the GTR filler and PU due to its higher concentration of low molecular weight compounds.

In this paper, GTR powder obtained from waste tire material recycles using mechanical grinding is used as filler to enhance the mechanical and physical properties of PU foam. In a first step, a series of structural and physical characteristics is performed in order to identify the composition as well as the physicochemical properties of the GTR powder. Then, a set of samples were made by incorporating the

TABLE 1 Procedure of fabricating polyurethane foams reinforced with treated ground tire rubber (GTR).

Solvent	Characteristics	GTR treatment	Rinsing and drying procedures
NaOH	Sodium hydroxide in the form of pellets, 98% purity	Immersion in 10% solution of NaOH for 2 h	Rinsing operation repeated three times, drying at 60°C during 24 h in oven
H <sub>2</sub> O <sub>2</sub>	Hydrogen peroxide with concentration of 30% in liquid phase stabilized by other additives	Addition in 30% solution of H <sub>2</sub> O <sub>2</sub> for 72 h	Rinsing operation repeated three times, drying at 70°C during 72 h in oven

FIGURE 1 Schematic procedure for fabricating polyurethane foams filled with pre-treated ground tire rubber. [Color figure can be viewed at [wileyonlinelibrary.com](http://wileyonlinelibrary.com)]

chemically pre-treated micrometric GTR powder in the PU matrix. The mixing process is conducted with variable GTR mass fractions according to free rising foam method.<sup>24</sup> The samples are then mechanically tested in compression at room temperature and their thermal stability is probed by thermogravimetry analysis (TGA). We further characterize the thermal conductivity and low frequency sound absorption coefficient measurements. It is also emphasized that the mechanical compressive properties are significantly enhanced compared to that of the pristine PU. Finally, we discuss the consequence of the GTR content on sound absorption and thermal conductivity performances in GTR/PU samples.

## 2 | EXPERIMENTAL

### 2.1 | Materials and processing

The GTR powder from Tyre Recycling Solutions (Switzerland) is used as received. The density and average particle size are respectively 1.08 g/cm<sup>3</sup> and 340.25 μm. A preliminary treatment is applied to increase the active surface area of the GTR powder in order to enhance the GTR/PU interfacial adhesion, the morphology stabilization, as well as the dispersion state.<sup>25,26</sup> For that purpose, an acid etching method based on suitable chemical modifier agent is used to chemically treat the

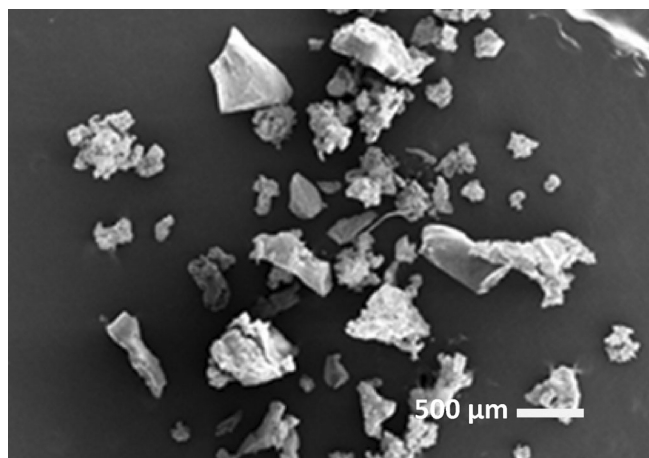


**FIGURE 2** The typical scanning electron microscopy picture of ground tire rubber powder obtained by mechanical grinding shows a large size distribution.

GTR powder. Two solvents are chosen: NaOH supplied by Alfa Aesar and H<sub>2</sub>O<sub>2</sub> supplied by VWR Chemicals (USA). For both cases, the protocols are listed in Table 1.

The treated powder is then embedded inside a thermoplastic PU foam polymer with different weight fractions. The PU resin is supplied by Smooth-On Inc. (USA) and is composed by two constituents: part A (4,4' methylenebis(phenylisocyanate), benzene, 1,1' methylenebis[4-isocyanato-], homopolymer, and methylenedi-phenyl diisocyanate with the respective mass fractions of 15–35, 5–10, and <1.5 wt%) and part B (mixture of polyol, blowing agent, catalysis, and surfactant). The GTR/PU composite foams are elaborated at room temperature by using free rising foam method (Figure 1).

This one-shot method is commonly used to fabricate flexible and rigid foams.<sup>27–29</sup> This method has the merit to operate at low temperature and to lead to reproducible properties.<sup>29</sup> It consists on mixing the two parts A and B with weight ratio 1A:2B. In the first step the treated powder content (5, 10, 15, and 20 wt%) is mixed with part A using a mechanical stirrer at 1440 rpm for 1 min. Then, the resulting mixture and part B are kept in a refrigerator for 20 min to delay the reaction time between two components. Next, they are mixed for 35 s and kept in cylindrical mold with 50 mm diameter for 24 h to cure.

## 2.2 | Methods

Density of the as-received GTR powder by pycnometer is done, with toluene as solvent. The nominal value of the density is obtained from  $\rho = \frac{M_2 - M_1}{(M_2 - M_1) - (M_3 - M_4)} \rho_t$ , where  $\rho_t$  denotes the density of toluene. In this equation,  $M_1$  represents the weight of the empty pycnometer,  $M_2$  is the

weight of the pycnometer filled with the GTR powder,  $M_3$  is the weight of the pycnometer filled with toluene, and  $M_4$  is the weight of the pycnometer containing both toluene and the GTR powder. The obtained value is 1.08 g/cm<sup>3</sup> that is comparable of the value measured for rubber powder with particle sizes ranging from 50 to 1000  $\mu\text{m}$ .<sup>30</sup>

The surface morphology of the GTR powder is characterized with LEO Gemini 1530 and JEOL JSM 6010 PLUS/LV scanning electron microscopy (SEM) under high vacuum. The GTR is initially metallized by tungsten and the applied voltage ranges from 2 to 5 kV. A typical image is shown in Figure 2. SEM observations reveal that particles are characterized by rough surfaces with irregular shapes and a wide size distribution from 20 to 698  $\mu\text{m}$ .

The particle size and distribution of GTR powder are analyzed using a MasterSizer<sup>®</sup> Laser-Diffraction Particle Size Analyzer (Mastersizer 3000, Malvern Instruments Ltd., Malvern, UK). For that purpose, 25 g of powder is placed on the powder disperser (Aero S) and subjected to laser light dispersion. Triplicate sample analysis is performed to obtain the size distribution curves and the percentile values  $D_{10}$ ,  $D_{50}$ , and  $D_{90}$  which indicate the size below which 10%, 50%, or 90% of all particles are found.

The surface area of the GTR powder is measured with the ASAP 2420 surface area analyzer using the Brunauer, Emmett, and Teller (BET) method (Micromeritics Instrument Corp., USA). CO<sub>2</sub> gas is utilized as adsorbate.

Identification of the polymer and composition of the GTR powder samples is performed by using x-ray diffraction (XRD) and Fourier transform infrared spectroscopy (FTIR). FTIR spectroscopy is carried out on a Bruker VERTEX 70 FTIR spectrometer. Acquisition is performed with wavenumber ranging from 600 to 4000 cm<sup>-1</sup>, averaged with 20 scans at a resolution of 2 cm<sup>-1</sup>. XRD patterns are recorded on an x-ray diffractometer EQUINOX 2000 using copper radiation CuK $\alpha$  ( $\lambda = 1.5418 \text{ \AA}$ ) at an accelerating voltage of 40 kV and an operating current of 30 mA in the range of  $2\theta$  (20–80°).

Additionally, TGA allows us to precise the percentage of each compound of the native GTR powder and measure the thermal stability of both GTR and GTR/PU samples. The thermal analysis is carried out using a NETZSCH 449 F3 Jupiter under two kinds of atmosphere, that is nitrogen and oxygen with a speed of 10°C/min using an Al<sub>2</sub>O<sub>3</sub> reference sample. The GTR powder is first heated from 30 to 600°C under nitrogen atmosphere, followed by switching the atmosphere to oxygen in order to determine the percentage of carbon black (CB) that can be located in the 600–1000°C temperature range. For GTR/PU samples, a NETZSCH5 is used between 30 and 900°C under a nitrogen flow keeping the same speed and reference sample as for the GTR powder.

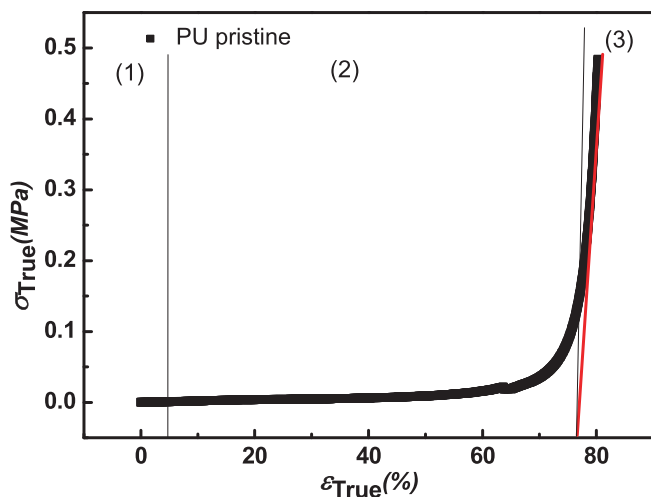


**FIGURE 3** Stress–strain response of pristine polyurethane polymer material under uniaxial compression at room temperature: (1) elastic, (2) plateau, and (3) densification regions. [Color figure can be viewed at [wileyonlinelibrary.com](https://onlinelibrary.wiley.com/doi/10.1002/app.56282)]

Room temperature compression tests are performed using GTR/PU samples with dimensions of  $20 \times 20 \times 10 \text{ mm}^3$ . The compression load cell, which is a cylindrical-shaped device with a mounting surface at the top and bottom ends, is essentially a transducer that converts force into an electrical signal. A maximum displacement of 10 mm is used, leading to a maximum force of about 105 N. The strain rate is set to 5 mm/min. A mechanical machine testing Instron Blue Hill series model is used and three samples are tested. A typical stress–strain curve is shown in Figure 3 for the pristine PU foam.

One can in fact separate this curve in three regions: (1) elastic, (2) plateau, and (3) densification. In the elastic region, the cell walls stretch elastically until collapse begin. Then, the cell buckling continues leading to the plateau region. During the densification stage, the PU foam acts as a solid material where the cell walls start to crush against each other causing a significant increase of the internal compression stiffness of the cellular network.<sup>31</sup>

The thermal conductivity of both GTR-PU samples and neat PU was determined using a Hot Disk 1500 instrument (Sweden) at room temperature. Semicircle samples with a 25 mm radius and 10 mm thickness are used. The Hot Disk sensor (Kapton 5465) is embedded within the samples and serves as heat source and temperature sensor. To measure the thermal conductivity, an output power set to 31.56 mW and a short measurement time (20 s) are applied for conducting samples.<sup>32</sup>

The acoustic absorption coefficient  $\alpha$  is determined using a Kundt tube. This system includes a speaker, two

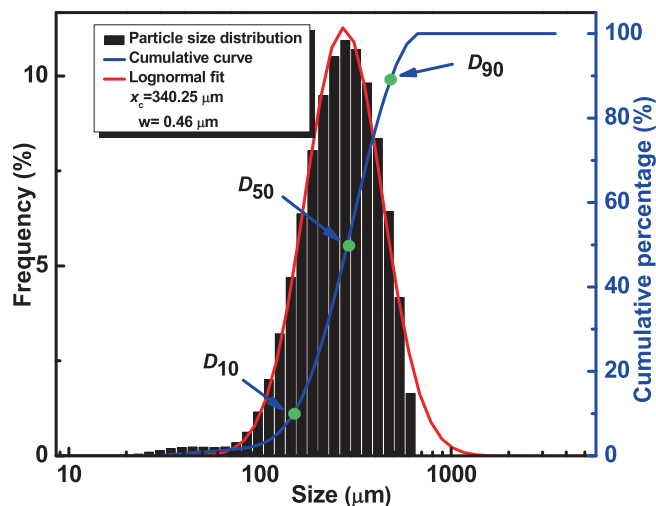


**FIGURE 4** Granulometric size distribution of ground tire rubber powder fitted by lognormal fit  $y = y_0 + \frac{A}{wx\sqrt{2\pi}} \exp\left(-\frac{\ln(\frac{x}{x_c})^2}{2w^2}\right)$  with average value  $x_c = 340.25 \mu\text{m}$  and standard deviation of  $0.46 \mu\text{m}$ . The parameters  $D_{10}$ ,  $D_{50}$ , and  $D_{90}$  are defined in the text. [Color figure can be viewed at [wileyonlinelibrary.com](https://onlinelibrary.wiley.com/doi/10.1002/app.56282)]

microphones and a digital frequency analyzer. This coefficient measures how much acoustic energy is absorbed by a sample relative to the energy incident upon it. Samples with diameter set to 50 mm and thickness of 10 mm are tested for frequencies ranging from 1000 to 4500 Hz.

## 3 | RESULTS AND DISCUSSION

### 3.1 | Recyclable waste tire characterizations

Figure 4 shows the granulometric distribution curve of the GTR powder. A broad size distribution of particles is observed, that is  $20 - 698 \mu\text{m}$ . Using a lognormal fit, we found that the average size of this distribution is  $340.25 \pm 0.46 \mu\text{m}$ .

We also obtained the percentile values  $D_{10} = 149 \mu\text{m}$ ,  $D_{50} = 286 \mu\text{m}$ , and  $D_{90} = 491 \mu\text{m}$ . Additionally, the  $D_{90}$  to  $D_{10}$  ratio characterizes the homogeneity degree of the GTR powder. In our case,  $\frac{D_{90}}{D_{10}} = 3.29 > 1$ , indicating a broad distribution.<sup>33</sup> The specific surface area of the GTR powder is about  $15.83 \text{ (m}^2/\text{g)}$  as measured using the BET method.

FTIR and XRD are also used to identify the chemical structure of the GTR powder. Figure 5 shows the FTIR spectrum of the GTR powder. Dominant bands are observed at (A)  $3438 \text{ cm}^{-1}$  and (H)  $1032 \text{ cm}^{-1}$  which are respectively assigned to the hydroxyl groups (OH)<sup>34</sup> and the Si–O–Si bond.<sup>35</sup> The high intensity of O–H

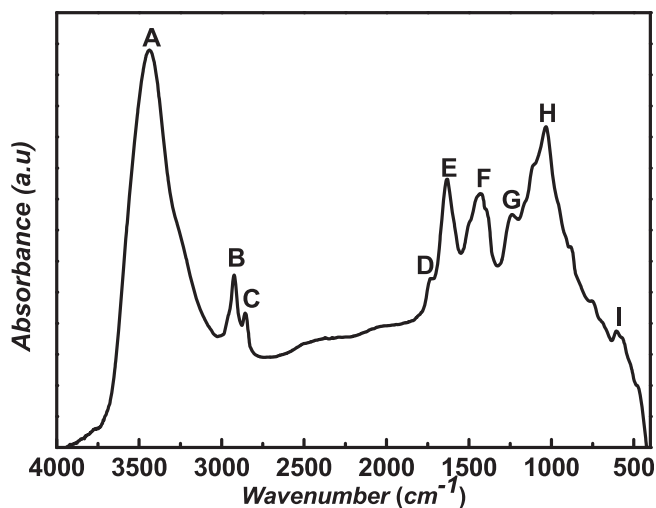


FIGURE 5 Fourier transform infrared spectroscopy spectrum of ground tire rubber powder with A-G peak assignment.

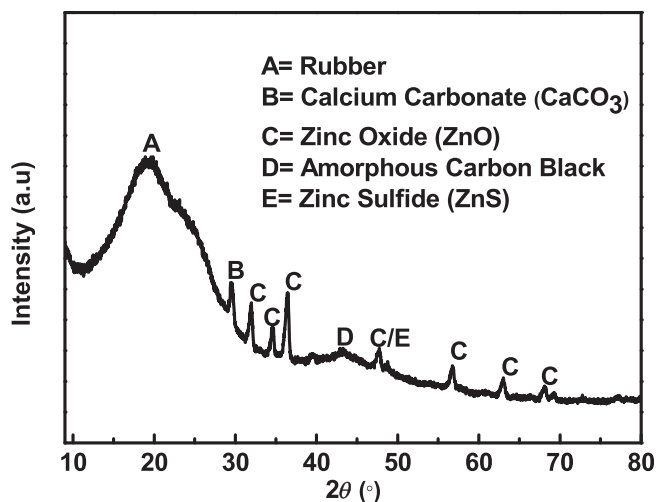


FIGURE 6 Room temperature XRD pattern of ground tire rubber powder.

groups is associated with the oxidation process. The peaks B, C, E and F located respectively at 2924, 2856, 1633, and 1433  $\text{cm}^{-1}$  are assigned in this order to the symmetric and asymmetric of C–H stretching vibration (B, C), the plane vibrating of aromatic =C–H and C=C (E), and the  $\text{CH}_2$  bending and aromatic stretching vibrations (F) of the styrene butadiene/natural rubber (SBR/NR). Other weak peaks (C, D, G, and I) can be also observed in Figure 5. For example, the peak G appearing at 1237  $\text{cm}^{-1}$  represents the C–O bond while the peak D located at 1727  $\text{cm}^{-1}$  refers to C=O and C=C alkene of CB as reported in.<sup>36</sup>

Figure 6 shows the room temperature XRD pattern of GTR powder with either narrow or broad peaks.

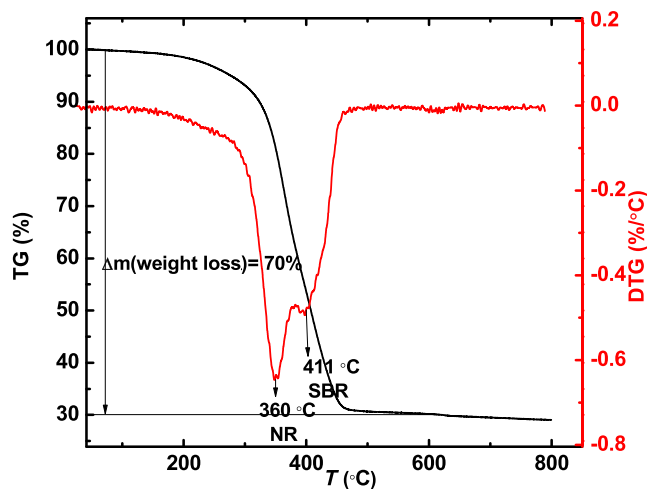


FIGURE 7 Thermogravimetry analysis curve (weight percentage versus temperature) of ground tire rubber powder determined at heating rate of 20°C/min and under nitrogen atmosphere. The derivative weight percentage (DTG) versus temperature curve is also plotted. [Color figure can be viewed at [wileyonlinelibrary.com](http://wileyonlinelibrary.com)]

The broad peak A located at 19° corresponds to rubber materials which can be composed by natural or synthetic rubbers like NR and SBR. The fraction composition of each rubber depends on the tire type, for example for a typical truck tire, a high fraction of NR (~37 wt%) is needed to increase the tire-fatigue resistance compared to a typical car tire (~21 wt%).<sup>4</sup> Several peaks designed by C are located at 31, 34, 36, 47, 56, 63, and 68° and are related to zinc oxide which used as accelerator of vulcanization process. The higher and lower intensities are respectively observed around 36 and 68°. At 29.5° we observe the peak B which corresponds to calcium carbonate  $\text{CaCO}_3$  used as filler in tire to enhance its structural strength and durability. The D broad peak corresponding to amorphous CB is centered at ~43.5°.

TGA is also used for a quantitative determination of the GTR powder composition.<sup>5</sup> The curve of weight change percentage as function of temperature and its derivative are plotted in Figure 7.

As can be seen, the powder shows a stable thermal behavior until ~250°C from which the weight loss starts to increase and reaches a maximal value around 70 wt% at ~411°C indicating a high degradation of the high volatile components of SBR and NR (oils, plasticizers, antioxidants) between 300 and 480°C. The remaining mass (30 wt%) is mainly composed by nonvolatile components (CB and ash). By changing the atmosphere environment (from nitrogen to oxygen), the mass fraction CB is then measured and found to be 28.78 wt%. This relatively high content suggests that CB was added to act as an efficient

**TABLE 2** Mechanical properties of polyurethane foam filled with ground tire rubber (GTR) treated by H<sub>2</sub>O<sub>2</sub> and NaOH at different contents and characterized under compression test.

Chemical treatment	GTR content (wt%)	<i>E</i> (kPa)	<i>R</i> <sup>2</sup>	$\sigma_{5\%}$ (kPa)	$\epsilon_{\text{onset}}$ (%)	UCS(MPa)	$\epsilon_b$ (%)
NaOH	0	14.24	0.98	0.81	77.52	0.48	80.3
	5	21.32	0.99	1.17	66.45	0.18	69.5
	10	20.47	0.99	1.13	63.56	0.51	67.5
	15	25.81	0.99	1.42	57.06	0.20	60.9
	20	26.06	0.99	1.4	59.85	0.49	63.7
H <sub>2</sub> O <sub>2</sub>	0	14.24	0.98	0.81	77.52	0.48	80.3
	5	14.43	0.99	0.80	57.96	0.48	61.0
	10	18.06	0.98	0.97	63.22	0.56	66.1
	15	24.55	0.97	1.39	62.03	0.50	65.5
	20	16.53	0.97	1	57.06	0.53	60.3

Abbreviation: UCS, ultimate compression strength.

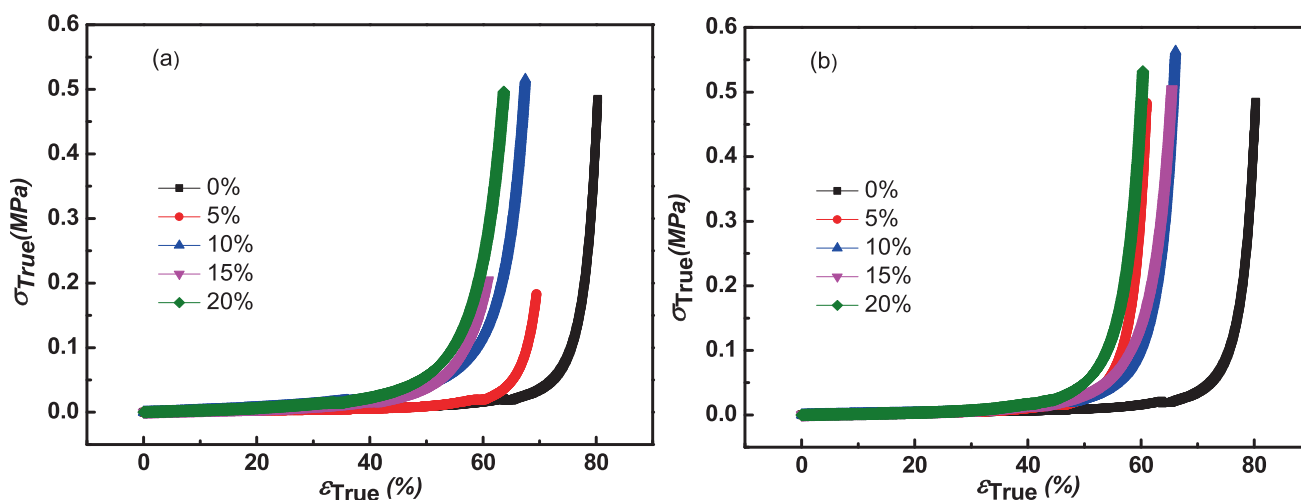


**FIGURE 8** (a) Stress–strain curves of neat and GTR/PU samples treated either by NaOH. (b) Same as in (a) for H<sub>2</sub>O<sub>2</sub> treatment. GTR, ground tire rubber. PU, polyurethane. [Color figure can be viewed at [wileyonlinelibrary.com](http://wileyonlinelibrary.com)]

barrier against the volatile organic components.<sup>37</sup> The overall composition of the powder as well as the maximum degradation temperature obtained from the derivative weight percentage (DTG) curve are listed in Table 2. We conclude that the actual composition is very close to that observed in similar powders.<sup>38,39</sup> In addition, the nominal values of the mass fraction of CB and NR suggest that they originate from heavy tires.<sup>38</sup>

### 3.2 | Properties of GTR/PU composites

With that in mind, we come to the main focus of our paper and discuss the thermal, mechanical as well as the acoustic properties of GTR/PU composites as function of the chemically pre-treated GTR content.

Figure 8 shows room temperature stress–strain curves under uniaxial compression as function of GTR weight percentage and chemical treatment used. Compatible with the generic behavior shown in Figure 3, we observe three distinct regions.

It is interesting to draw several conclusions. Firstly, the mechanical properties of GTR/PU samples are significantly enhanced compared to the neat PU foam indicating a good compatibility at the GTR/PU interfaces.<sup>23</sup> In addition, the reinforcing effect of the GTR powder can be connected to a significant drop of the PU porosity. To quantify this parameter, the onset densification  $\epsilon_{\text{Onset}}$  occurring at the third stage is considered. The results shown in Table 2 indicate a notable decrease of  $\epsilon_{\text{Onset}}$  from 77.52% corresponding to the pristine PU matrix to 56%–66% for all GTR/PU samples with GTR treated



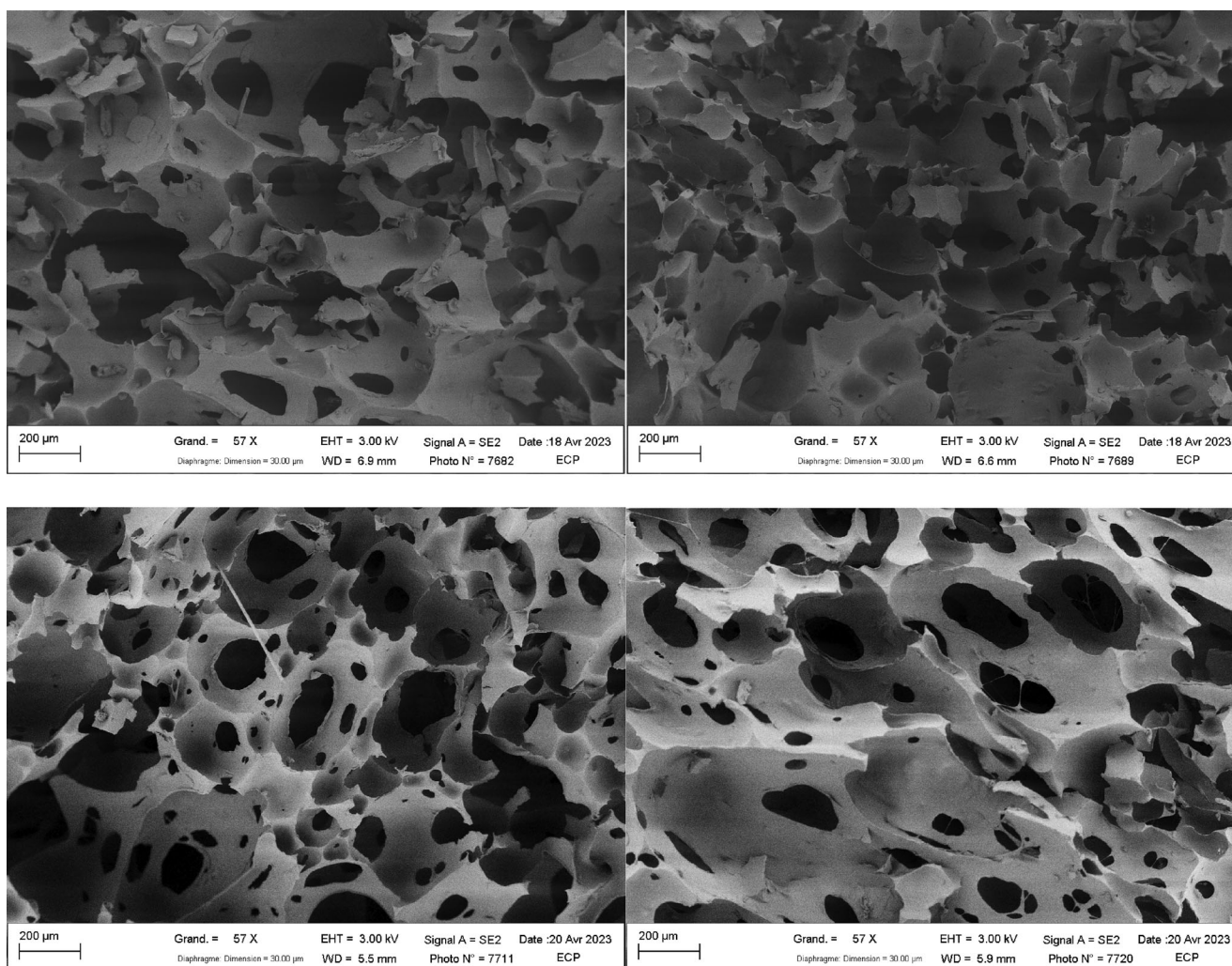
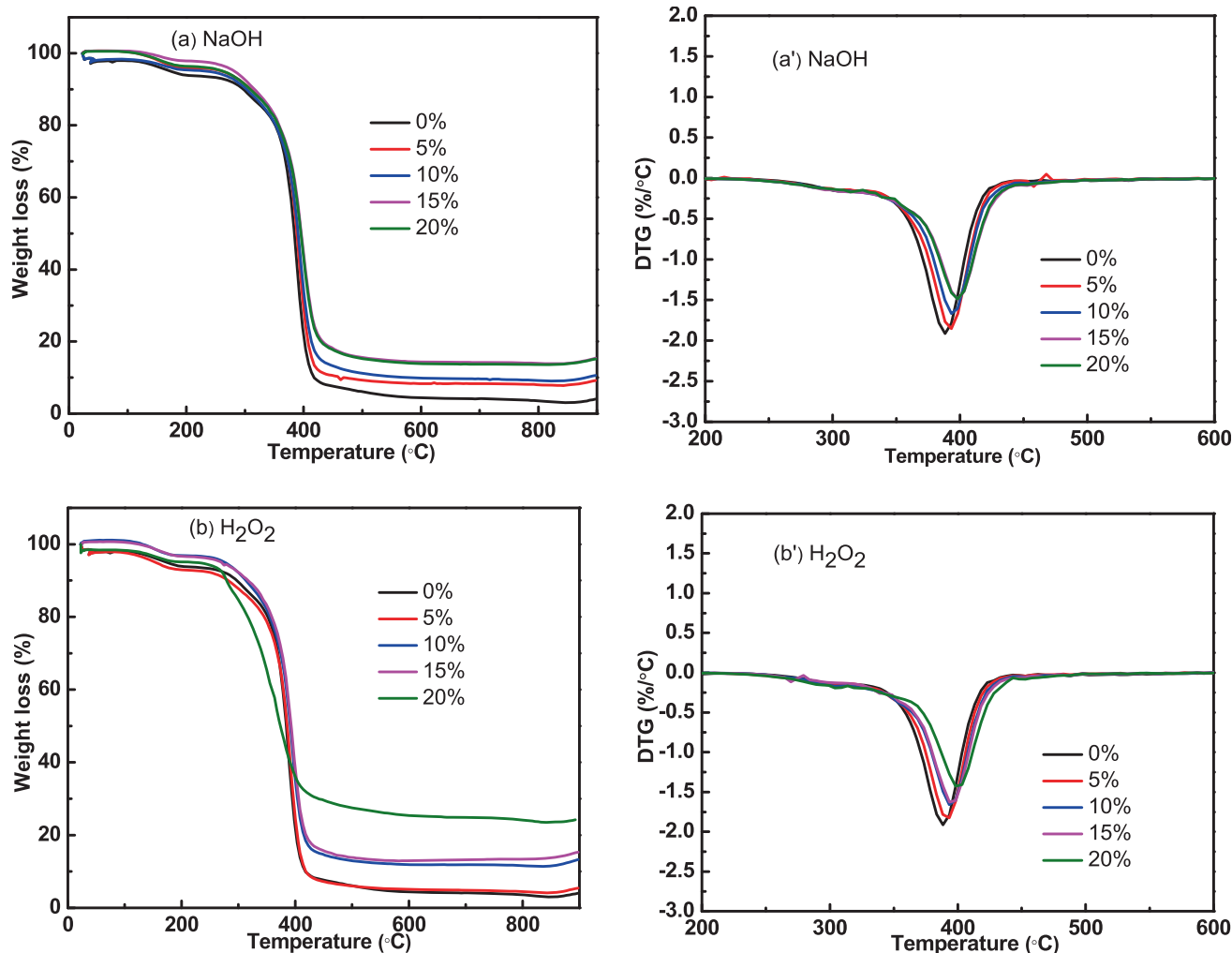


FIGURE 9 Typical scanning electron microscopy images of GTR/PU samples containing 5 (left) and 15 (right) wt% of ground tire rubber (GTR) chemically treated either by  $\text{H}_2\text{O}_2$  or NaOH, respectively. PU, polyurethane.

either with  $\text{H}_2\text{O}_2$  or NaOH. Thence, the mechanical properties of the PU matrix including ultimate compression strength (UCS) and Young modulus are enhanced as reported in Table 2. In parallel, an expected decrease of the ductility of the PU matrix measured by the deformation at break  $\epsilon_b$  is observed.<sup>40</sup> The observed reduction of  $\epsilon_{Onset}$  suggests an increase in the apparent density of the composite samples with a drop of open cell proportion as reported by Hejna and coworkers for flexible PU filled with ground tire rubber treated by  $\text{H}_2\text{O}_2$ .<sup>25</sup> The authors highlight that the chemical treatment creates higher interfacial interactions due to a reduction of the level of foam volumetric expansion therefore improving the compression strength of the composite. For the case of NaOH treatment, a similar mechanical behavior is observed because the NaOH removes zinc stearate from rubber surface by substituting zinc ions to sodium ions which are more soluble and can be easily removed by rinsing.

Note that the presence of zinc stearate causes poor adhesion with the matrix.<sup>41</sup> As can be also seen in Figure 8, the mechanical properties of the series of GTR/PU for samples are enhanced when the filler amount increases from 10 to 20 wt% for both chemical modifications applied on the GTR particles indicating good interfacial compatibility between the matrix and filler. However, the PU samples filled with 5 and 15 wt% show an opposite trend between the NaOH and  $\text{H}_2\text{O}_2$  treatments. For the case of NaOH treatment, the onset densification of the GTR/PU samples is significantly reduced as the GTR amount increases from 5 to 15 wt% but both filled PU samples exhibit practically the same UCS, that is 0.18–0.20 MPa (Table 2). When  $\text{H}_2\text{O}_2$  is used, the mechanical properties of the corresponding samples are improved especially for the UCS, that is 0.43–0.48 MPa associated to a reduction of  $\epsilon_{Onset}$  for PU filled with only 5 wt% of GTR. These differences in mechanical responses are



**FIGURE 10** Plots of (a, b) weight loss and (a', b') corresponding differential thermogravimetry analysis curves of foams containing (a, a') NaOH treated ground tire rubber (GTR) or (b, b') H<sub>2</sub>O<sub>2</sub> treated GTR. [Color figure can be viewed at [wileyonlinelibrary.com](https://onlinelibrary.wiley.com/doi/10.1002/app.56282)]

related to the cell morphology of the PU foam and its modification by the filler particles and the dispersion state in the PU matrix.<sup>42</sup>

The right-hand (resp. left-hand) side of Figure 9 shows typical SEM images for PU filled with respectively 5 and 15 wt% of GTR treated by NaOH (resp. H<sub>2</sub>O<sub>2</sub>).

For H<sub>2</sub>O<sub>2</sub> treated GTR/PU samples, we observe a uniform structure associated to an increase of partially open pores as the filler increases. The fineness of pores and cavities for PU sample containing 5 wt% of GTR which is clearly visible compared to that containing 15 wt% of GTR explain their higher mechanical properties which is consistent with the study reported by Hejna and coworkers<sup>25</sup> using H<sub>2</sub>O<sub>2</sub> treated GTR in PU foam. On the other hand, for NaOH treated GTR/PU samples, we observe that despite the drop of the open pores as the filler increases, the microstructure is less uniform due to the presence of agglomerates and defects, thus reducing their mechanical characteristics.

To sum up, the general trend shows that the PU samples containing 20 wt% of GTR have better a mechanical behavior whatever the chemical treatment used. In particular, high compression strength can be used as a metric for good durability of the PU foam.<sup>43</sup> We note that comparable performances can be reached by adding only 5 wt% of GTR particles when they are treated by using H<sub>2</sub>O<sub>2</sub>. However, for environmental purposes the use of high content of waste tire material recycles is preferred.

The curves of weight change percentage as function of temperature and their derivatives are reported in Figure 10.

All GTR/PU samples exhibit an improvement of their thermal stability as GTR content is increased. This result is due to some constituents of the filler, especially CB ( $\cong 29\%$ ) as extracted from TGA experiments (Figure 7). For comparison purposes, the effect of the filler on the thermal stability is more pronounced for the series of H<sub>2</sub>O<sub>2</sub> treated GTR/PU samples. Table 3 summarizes the

**TABLE 3** Thermogravimetry analysis of neat and GTR/PU samples for different ground tire rubber (GTR) contents treated with NaOH and H<sub>2</sub>O<sub>2</sub>.

Samples	GTR content (wt%)	Residue (wt%)	$T_{\max}$ (DTG)	Thermal conductivity (W/mK)
NaOH	0	4.04	388.44	0.020
	5	9.22	393.39	0.024
	10	10.62	393.34	0.025
	15	15.38	398.32	0.026
	20	15.19	398.26	0.025
H <sub>2</sub> O <sub>2</sub>	0	4.04	388.44	0.020
	5	5.45	393.31	0.0244
	10	13.31	393.36	0.0251
	15	15.30	393.48	0.0242
	20	24.24	398.35	0.0238

Abbreviations: DTG, derivative weight percentage; PU, polyurethane.

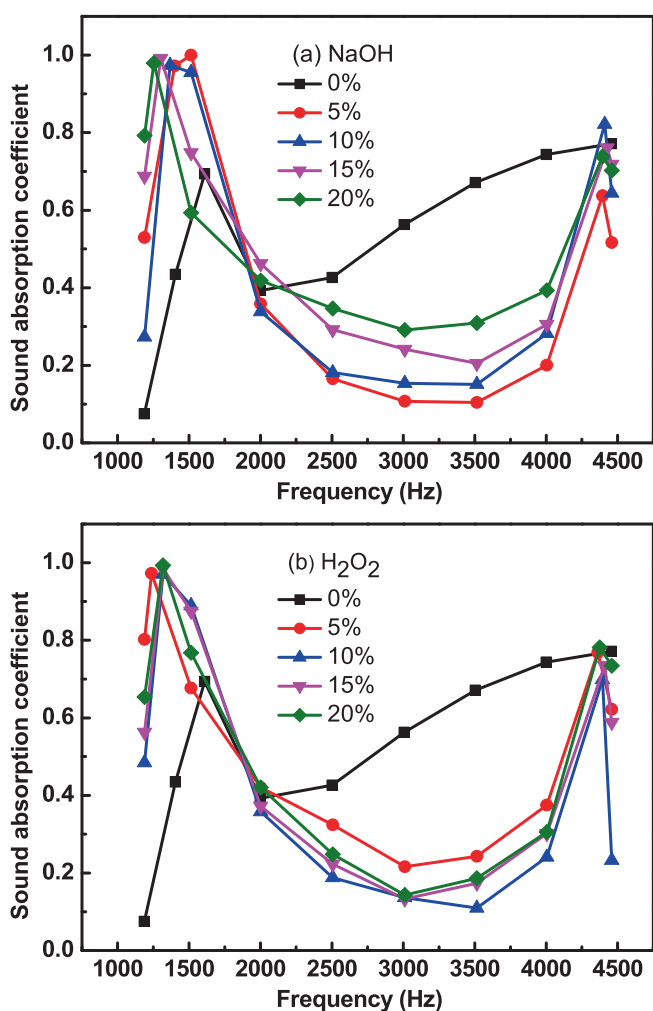


**FIGURE 11** (a) The spectral variation of sound absorption coefficient of neat and PU-GTR samples treated either by NaOH. (b) Same as in (a) with H<sub>2</sub>O<sub>2</sub> treatment. GTR, ground tire rubber. PU, polyurethane. [Color figure can be viewed at [wileyonlinelibrary.com](http://wileyonlinelibrary.com)]

variation of these physical quantities as function of filler content.

We observe that for the treated H<sub>2</sub>O<sub>2</sub> GTR/PU sample containing 20 wt% of GTR, the nominal value recorded of the residual value (i.e. 24.24 wt%) is significantly larger than the corresponding value for the NaOH treated GTR/PU sample (i.e. 15.19 wt%). Referring to the above discussed mechanical response, it is concluded that highly filled GTR/PU with H<sub>2</sub>O<sub>2</sub> treated GTR is characterized by both high thermal stability and compression strength.

Now we move to the sound absorption characteristics of GTR/PU samples. The obtained spectra (Figure 11) allow to distinguish the three spectral ranges as a result of incorporating pre-treated GTR particles in PU (Table 4).

Firstly, in the 3rd range (3515–4459 Hz), the sound absorption coefficient  $\alpha$  is very close to the corresponding value of pristine PU. However, we observe a significant increase of  $\alpha$  from the 2nd range (2001–3515 Hz) to the 1st range (1188–2001 Hz) when GTR particles are added to the pristine PU. This behavior is consistent with earlier findings reported in the literature for similar materials.<sup>44,45</sup> Two main mechanisms: (i) air-flow resistivity and (ii) tortuosity which are closely dependent on the open porosity were invoked.<sup>44–46</sup> These mechanisms provide longer residence time and higher number of collisions for the sound waves with air molecules and matrix walls at low frequencies. Recent work<sup>45</sup> has claimed that increasing residence time has for effect to increase the maximum value of  $\alpha$  and the frequency corresponding to this maximum decrease when the tortuosity increases. Indeed, the air-flow resistivity contributes to increase the absorption performance throughout the resistance experienced by air molecules when they pass through open

**TABLE 4** Sound absorption coefficient for samples with different ground tire rubber (GTR) contents treated with NaOH and H<sub>2</sub>O<sub>2</sub>.

Sample	GTR (wt%)	Sound absorption coefficient ( $\alpha$ )		
		1st range	2nd range	3rd range
		1188–2001 Hz	2001–3515 Hz	3515–4459 Hz
PU/GTR <sub>-NaOH</sub>	0	0.15	0.7	0.73
	5	0.99	0.1	0.64
	10	0.97	0.12	0.82
	15	0.99	0.2	0.76
	20	0.98	0.27	0.74
PU/GTR <sub>-H<sub>2</sub>O<sub>2</sub></sub>	5	0.97	0.21	0.78
	10	0.97	0.1	0.69
	15	0.98	0.13	0.73
	20	0.99	0.14	0.78

Abbreviation: PU, polyurethane.

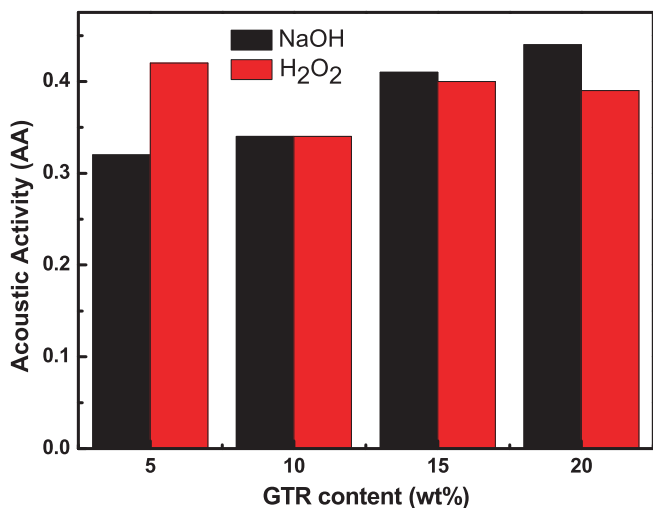


**FIGURE 12** Effect of the chemical treatment (NaOH and H<sub>2</sub>O<sub>2</sub>) on the acoustic activity (AA) of PU-GTR composites for different mass fractions of ground tire rubber (GTR). PU, polyurethane. [Color figure can be viewed at [wileyonlinelibrary.com](http://wileyonlinelibrary.com)]

pores in the porous composite.<sup>47</sup> The viscoelastic character of the GTR powder has also an important effect on these changes<sup>48,49</sup> since the incident energy can be partly absorbed by scattering from the CB particles contained in the GTR powder (Figure 7). The presence of the GTR including CB particles increases the tortuosity by reducing the porosity as discussed above. In fact, it is expected that tortuosity mostly affects the location of the quarter-wavelength point for which the path length in porous materials coincides with the quarter-wavelength of the incident sound energy.<sup>50,51</sup> Thus, the increased quarter-wavelength point at high tortuosity shifts the sound absorption peak to the lower-frequency region.<sup>45</sup> It should be noted that the thermal characteristic length

parameter does not affect the absorption process since the thermal conductivity of the PU matrix is only slightly changed by addition of GTR powder (Table 3). Overall, this experimental result reflects the signature of the thermal insulator character of both series of PU-GTR composites studied in this work.

Figure 12 compares the average sound absorption coefficient (acoustic activity) for both PU-GTR samples according to the chemical treatment used (NaOH or H<sub>2</sub>O<sub>2</sub>) determined in the entire range of frequencies.<sup>52</sup>

Overall, the results indicate a relatively similar response for PU samples containing 10 and 15 wt% for which the obtained values of acoustic activity (AA) coefficient are closed to 0.33 and 0.40 respectively. However, the chemical treatment by H<sub>2</sub>O<sub>2</sub> leads to a larger value of AA (0.42) for PU filled with only 5 wt% compared to the value with the NaOH treatment. This result is consistent with the good compression behavior obtained for that sample (Figures 8 and 9 and Table 2) owing to its pore size and distribution inside the PU matrix. Furthermore, this trend is opposite for the sample containing 20 wt% of GTR. Thence, features of the chemical treatment of GTR put constraints on what the content of open porosity in these PU-based samples may be.<sup>45</sup>

We should say that the observed behavior can have great potential in engineering applications for which challenges in achieving perfect absorption at sub-wavelength scales is crucial, for example underwater acoustics.<sup>53,54</sup> For instance, Zhong and coworkers<sup>54</sup> proposed a new super-material plate for underwater sound absorption made by a combination of CB filled PU and a square lattice of spiral resonator. This ultrathin structure shows an average sound absorption coefficient of 0.54 in the broad frequency range (800–6000 Hz) under atmospheric pressure conditions with low frequency

absorption capacity and resistance to high hydrostatic pressure. The most important takeaway is that the correlation between the mechanical and acoustic performances is crucial to prevent structural damage or instability of the PU polymer structures during vibration ensuring hence their normal operation.<sup>53</sup>

## 4 | CONCLUSION AND OUTLOOK

In conclusion, one seems justified in asserting that the mixing of GTR particles in PU foam enhances the physical and mechanical properties of the pristine PU matrix. Our results indicate an enhancement in the compression behavior compared to the neat PU. The thermal stability is also improved especially for samples for which the GTR particles are pre-treated with H<sub>2</sub>O<sub>2</sub>. Additionally, the data presented in this paper show a good correlation between the thermal and mechanical properties. As noted already, this specific behavior is related to the small pore sizes and their uniform dispersion in the PU. It should perhaps be emphasized once again that the good acoustic absorption of these composites at low frequencies reflects the simultaneous increase of the air-flow resistivity and tortuosity by the GTR particles. This is clearly of great interest in the field of underwater acoustics.

There do of course remain a number of points to be investigated, regarding the multifunctionality issue of the GTR/PU composites. One important question in this regard is how to optimize the foam composite fabrication with a uniformly distribution of small pores and cavities. It would seem very desirable to better control the many degrees of freedom of the GTR powder, for example size, finesse, composition, since they eventually impact the final performance of the foam composite.

### AUTHOR CONTRIBUTIONS

**Y. Nezili:** Investigation (equal); software (equal); visualization (equal). **I. El Aboudi:** Conceptualization (equal); resources (equal); software (lead); validation (equal). **D. He:** Conceptualization (equal); investigation (equal); resources (equal); writing – original draft (equal). **A. Mdarhri:** Conceptualization (equal); investigation (equal); resources (equal); validation (equal); writing – original draft (equal). **C. Brosseau:** Supervision (equal); validation (equal); writing – review and editing (equal). **M. Zaghrioui:** Investigation (equal); resources (equal); writing – original draft (equal). **T. Chartier:** Investigation (equal); software (equal). **A. Ghorbal:** Investigation (equal); software (equal). **R. Ben Arfi:** Investigation (equal); software (equal). **J. Bai:**

Conceptualization (equal); resources (equal); validation (equal); writing – review and editing (equal).

### ACKNOWLEDGMENTS

This work was funded by Ministère de l'Enseignement Supérieur, de la Coopération Scientifique et de l'Innovation, (MERCISI-Morocco) and Agence Universitaire Francophone (AUF) in the framework of the convention AUF 2021 N° DRM-6871. The authors and especially Y.N. would like to acknowledge MERCISI and AUF for financial support. Partial funding is also provided by LMP from Université de Paris-Saclay (UPS), France.

### CONFLICT OF INTEREST STATEMENT

The authors declare that they have no known competing financial interests or personal relationships that could have appeared to influence the work reported in this paper.

### DATA AVAILABILITY STATEMENT

The data that support the findings of this study are available from the corresponding author upon reasonable request.

### ORCID

C. Brosseau  <https://orcid.org/0000-0002-2629-0267>

### REFERENCES

- [1] I. El Aboudi, A. Mdarhri, Y. Nezili, C. Brosseau, *Elastomers in Engineering Applications* (Ed: S. Thomas), Springer, Berlin, Germany **2024**.
- [2] A. Hejna, P. Kosmela, A. Olszewski, Ł. Zedler, K. Formela, K. Skórczewska, A. Piasecki, M. Marć, R. Barczewski, M. Barczewski, *Environ. Sci. Pollut. Res.* **2024**, *31*, 17591.
- [3] L. Yang, Y. Xiang, Y. Li, W. Bao, F. Ji, J. Dong, J. Chen, M. Xu, R. Lu, *AIP Adv.* **2023**, *13*, 75024.
- [4] F. Valentini, A. Pegoretti, *Adv. Ind. Eng. Polym. Res.* **2022**, *5*, 203.
- [5] K. Formela, *Adv. Ind. Eng. Polym. Res.* **2022**, *5*, 255.
- [6] J. Thomas, R. S. Patil, M. Patil, J. John, *Sustainability* **2023**, *15*, 15758.
- [7] L. E. Alonso Pastor, K. C. Núñez Carrero, J. Araujo-Morera, M. Hernández Santana, J. M. Pastor, *Polymer* **2021**, *14*, 11.
- [8] X. Zhang, Z. Lu, D. Tian, H. Li, C. Lu, *J. Appl. Polym. Sci.* **2012**, *127*, 4006.
- [9] R. Ružickij, O. Kizinievič, R. Grubliauskas, T. Astrauskas, *Sustainability* **2023**, *15*, 2799.
- [10] A. Hejna, J. Koro, M. Przybysz-Romatowska, Ł. Zedler, B. Chmielnicki, K. Formela, *Waste Manage.* **2020**, *108*, 106.
- [11] M. Peng, S. Jianbo, X. Dong, D. Guanhong, *Advances in Sustainable Manufacturing*, Springer, Berlin, Germany **2011**, p. 261.
- [12] Z. Xiao, A. Pramanik, A. K. Basak, C. Prakash, S. Shankar, *Cleaner Mater.* **2022**, *5*, 100115.
- [13] V. Spanheimer, G. G. Jaber, D. Katrakova-Krüger, *Polymer* **2023**, *15*, 2174.

- [14] P. K. De Maeijer, B. Craeye, J. Blom, L. Bervoets, *Infrastructures* **2021**, 6, 116.
- [15] B. K. Saleh, M. H. Khalil, *Egypt. J. Chem.* **2017**, 60, 1205.
- [16] R. Maderuelo-Sanz, J. M. Barrigón Morillas, M. Martín-Castizo, V. Gómez Escobar, G. Rey Gozalo, *Lat. Am. Appl. Res.* **2013**, 10, 585.
- [17] A. Verma, K. Baurai, M. R. Sanjay, S. Siengchin, Mechanical, microstructural, and thermal characterization insights of pyrolyzed carbon black from waste tires reinforced epoxy nanocomposites for coating application, polymer composites. **2020**, 41, 338.
- [18] S. Ubaidillah, F. Imaduddin, Y. Li, S. A. Mazlan, J. Sutrisno, T. Koga, I. Yahya, S. B. Choi, *Smart Mater. Struct.* **2016**, 25, 115002.
- [19] J. O. Akindoyo, M. D. H. Beg, M. R. Suriati Ghazali, N. J. Islam, A. R. Yuvaraj, *Advances* **2016**, 6, 114453.
- [20] W. Witkiewicz, A. Zieliński, *Adv. Mater. Sci.* **2006**, 6, 35.
- [21] M. Cerny, J. Jancar, *Chem.* **2017**, 71, 1119.
- [22] H. Olcay, E. D. Kocak, *J. Ind. Text.* **2022**, 51, 8738.
- [23] P. P. Kosmela, A. Olszewski, L. Zedler, P. Burger, A. Piasecki, K. Formela, A. Hejna, *Materials*, **2021**, 14, 3807.
- [24] R. Gayathri, R. Vasanthakumari, C. Padmanabhan, *Int. J. Sci. Eng. Res* **2013**, 4, 301.
- [25] A. Hejna, A. Olszewski, Ł. Zedler, P. Kosmela, K. Formela, *Materials* **2021**, 14, 499.
- [26] X. Colom, F. Carrillo, J. Cañavate, *Compos. Pt. A-Appl. Sci. Manuf.* **2007**, 38, 44.
- [27] G. Wegrzyk, D. Grzeda, J. Ryszkowska, *Materials* **2023**, 16, 16020857.
- [28] S. Suleman, S. M. Khan, N. Gull1, W. Aleem, M. Shafiq, T. Jamila, *Int. J. Innov. Sci.*, **2014**, 12, 165.
- [29] P. K. Huester, D. P. Huntington, *J. Cell. Plast.* **1965**, 1, 301.
- [30] A. Fazli, D. Rodrigue, *Recycling* **2021**, 6, 44.
- [31] M. H. Moghim, M. Keshavarz, S. M. Zebarjad, *Polym. Bull.* **2019**, 76, 227.
- [32] D. S. W. Pau, C. M. Fleischmann, M. J. Spearpoint, K. Y. Li, *Fire Mater.* **2014**, 38, 433.
- [33] J. Araujo-Morera, R. Verdugo-Manzanares, S. González, R. Verdejo, M. A. Lopez-Manchado, M. Hernández Santana, *J. Compos. Sci.* **2021**, 5, 68.
- [34] A. Belgacem, M. Belmedani, R. Rebiai, H. Hadoun, *Eng. Trans.* **2013**, 32, 1974.
- [35] Ł. Zedler, X. Colom, M. Reza Saeb, K. Formela, *Composites, Part B* **2018**, 145, 182.
- [36] A. S. Abdulrahman, F. H. Jabrail, *Recycling* **2022**, 7, 27.
- [37] F. Niknam, The science behind tread depth on passenger tires. <https://www.tirereview.com/science-behind-tread-depth-passenger-tires/> **2021**.
- [38] Z. Hrdlička, J. Brejcha, J. Šubrt, D. Vrtiška, L. Malinová, D. Čadek, A. Kadeřábková, *Plast., Rubber Compos.* **2022**, 51, 497.
- [39] Japan Automobile Tyre Manufacturers Association, Tyre LCCO2 calculation guidelines ver.3.02021. [https://www.bridgestone.com/responsibilities/environment/reduce\\_co2/pdf/lcco2guidelines.pdf](https://www.bridgestone.com/responsibilities/environment/reduce_co2/pdf/lcco2guidelines.pdf)
- [40] F. Elhaouzi, A. Mdarhri, C. Brosseau, I. El Aboudi, A. Almaggoussi, *Polym. Bull.* **2018**, 76, 2765.
- [41] M. Nuzaimah, S. M. Sapuan, R. Nadlene, M. Jawaid, *Appl. Sci.* **2020**, 10, 3913.
- [42] D. Yun, J. H. Kim, *Adv. Powder Technol.* **2024**, 35, 104349.
- [43] G. Sung, J. S. Kim, J. H. Kim, *Polym. Adv. Technol.* **2017**, 29, 1.
- [44] J. Lee, J. H. Kim, *Polym. Test.* **2023**, 124, 108069.
- [45] H. Choe, G. Sung, J. H. Kim, *Compos. Sci. Technol.* **2018**, 156, 19.
- [46] F. Fahy, D. Thompson, *Noise Control, Fundamentals of Sound and Vibration*, 2nd ed., CRC Press, London, **2015**, p. 213.
- [47] L. Cao, Q. Fu, Y. Si, B. Ding, J. Yu, *Communications* **2018**, 10, 25.
- [48] S. M. Chen, Y. Jiang, J. Chen, D. F. Wang, *Adv. mater. sci. eng.* **2015**, 2015, 317561.
- [49] A. H. Baferani, A. A. Katbab, A. R. Ohadi, *Eur. Polym. J.* **2017**, 90, 383.
- [50] K. V. Horoshenkov, M. J. Swift, *Appl. Acoust.* **2001**, 62, 665.
- [51] H. S. Seddeq, *Aust. J. Basic Appl. Sci.*, **2009**, 3, 4610.
- [52] W. N. Fauziyah, A. Z. Irmansyah, S. Purwani, *Int. J. Simul. Model.* **2021**, 2, 117.
- [53] W. Kong, T. Fu, T. Rabczuk, *Appl. Acoust.* **2024**, 221, 110011.
- [54] H. Zhong, Y. Gu, B. Bao, Q. Wang, J. Wu, *Compos. Struct.* **2019**, 220, 1.

**How to cite this article:** Y. Nezili, I. El Aboudi, D. He, A. Mdarhri, C. Brosseau, M. Zaghrioui, T. Chartier, A. Ghorbal, R. B. Arfi, J. Bai, *J. Appl. Polym. Sci.* **2024**, e56282. <https://doi.org/10.1002/app.56282>